Lymph node swelling combined with temporary effector T cell retention aids T cell response in a model of adaptive immunity

Supplementary File 1 : Supplementary Methods A

1.1 LN geometry and swelling

Paracortical areas are defined using a percentage of the outer radius (Fig A i). Entry areas are defined as grid compartments within 50% of the outer radius in accordance with HEV positioning [1]. Grid compartments are designated exit compartments in an area with thickness 7% of the outer radius. A cap shaped area void of exit points is defined using 70% of the radius. The boundary region is one grid compartment thick and all grid compartments outside this region are defined as 'outside'.

In repastSimphony a 'valueLayer' is a parallel grid that stores a value for each grid-compartment that agents can access. For example, an entry area is designated a value of 24, and a region that is neither entry, exit, boundary or outside is designated a value of 20. Definition occurs during initialisation (line 70 lymph_nodeBuilder) and every 10 time-steps (line 446 lymph_node3DContext). A cylindrical entry region, with radius 30% of the outer radius, representing T cell (TC) entry from afferent lymphatics is defined in function addAfferent (line 941 lymph_node3DContext).

A sigmoidal relationship was estimated between paracortical volume and number of TCs present, based on patterns of behaviour recorded in Table A. To implement these changes, area represented by each grid compartment could be redefined using the new desired outer radius.

Fig A Modelling Methods. (i). Definitions of different areas of the paracortex are based on the overall paracortical radius, and therefore alter in volume during expansion. (ii). During interactions, TCs gain stimulation at a rate proportional to the presented antigenic signal, which is itself decaying. Accumulated TC simulation also undergoes constant decay. (iii). Accumulated stimulation is to determine probability of TC activation or differentiation, dependent on the satisfaction of other criteria.(iv) The progression of TC proliferation and differentiation into effector and long-lived memory TCs with sufficient stimulation.

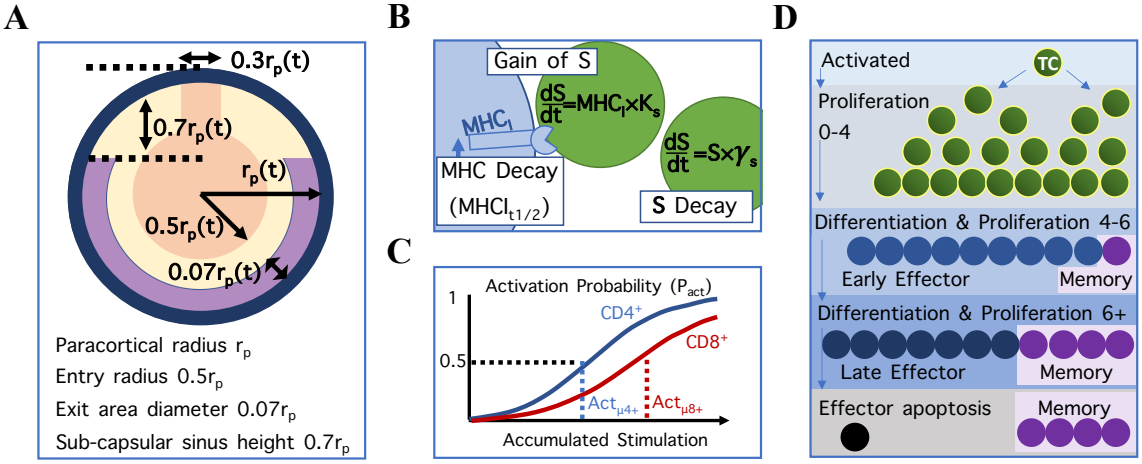

Table A Data regarding changes in lymphocyte counts and proliferation, LN mass, LN volume, blood flow and stromal cell counts and proliferation were collected from a range of sources and analysed to identify common relationships between T cells and LN volume.

Description	Stimuli	Model	Reference
LN mass, T cells, B cells, lymphocytes, total cellularity, Blood Endothelial Cells, migratory DCs, FRCs	Hindpad CFA/OVA injection	murine	[2]
LN volume, HEV length, LN images	Hindpad CFA/OVA injection	murine	[3]
LN volume, HEV length, B cell volume,	Hindpad LCMV injection	murine	[4]
LN images, Dendritic cells, endothelial cell proliferation, total LN cellularity, HEV proliferation	LPS-matured BMDC injection	murine	[5]
LN mass, peripheral blood T cells ($CD4^+$ /$CD8^+$), lymphocytes, T cell $CD4^+$, T cell $CD8^+$	skin-application of dinitrofluorobenzene	murine	[6]
LN blood flow, LN weight, lymphocyte influx, HEV proliferation, cell proliferation	sheep erythrocytes	rat	[7]
LN total cell count, blood flow T cells (CD4+/CD8+), B cells, T cell proliferation, B cell proliferation	HCpG/LPS +/- OVA also HSV	murine	[8]
LN cellularity, FRCs, LECs, BECs, T cells (CD4+/CD8+), FRC/LEC/BEC proliferation	OVA/Mont-immunized	murine	[9]

1.2 TC recruitment

Under non-inflammatory conditions, it was assumed that TC entry and exit remain constant and TCs occupy a constant percentage (55%) of total paracortical volume.Our hemispheric model has a radius of 200μm and average TC volume is assumed to be 150μm^2, resulting in approximately 50000 TCs at initiation. Scaling paracortical radius to paracortical radius in LN images, we estimate that the model represents a LN of 0.113-0.268 mm^3, implying a LN mass of 0.18-0.44mg (based on collaborative unpublished measurements of murine popliteal LN mass versus volume). Reported lymphocyte recruitment for a popliteal LN of 1.15g is $4x10^7$ lymphocytes/hour and up to 40% of lymphocytes are B cells [10–12]. The model represents half a paracortex, therefore TC recruitment rate was estimated as 1950-9000 TCs/hour under non-antigenic conditions. Naive TC transit time through the LN (T_{res}) was estimated as 6-24 hours [13].

1.3 Agents and agent migration

The agents were designated as members of the TC or DC class each containing individual properties (eg. age) that are updated each timestep (Fig C). Agent properties such as life-span and size are fixed parameters displayed in Table B.

The starting TC population is composed of 70% helper TCs ($CD4^+$) and 30% cytotoxic TCs ($CD8^+$) [14]. Each timestep (δt=20s), TCs can move one grid length to an available neighbouring

grid compartment, moving with probability, β, and where availability is governed by crowding parameter γ. TC migration was assumed to follow a random walk with pauses. Previous models have described TC migration with Brownian motion, a random-walk with persistence,run and tumble, and Lévy walks amongst other methods, partly due to differing reports of *in-vivo* migration. [15–18].

DC entry rate and total number was scaled from counts of migrating DCs and initial TCs in a murine LN post-immunisation [2]. Total number of DCs to enter at default was estimated as 4% of T cells present (ϕ_{DC}=0.05), therefore approximately 2500 DCs. Simulated DCs appear at points throughout the initial paracortex, at a constant entry rate for 2 days, with entry rate subsiding over the following 12 hours. Each DC has an average life span of 60 hours (+/-2.7h), after which the DC undergoes apoptosis and is removed from the model.

1.4 Agent interaction and signal integration

Interaction times with agDCs are drawn from uniform probability distributions with a mean of 3 minutes for non-cognate TCs (T_{NC}). Cognate TCs progress from 10-15 minute short interactions (T_{short}) to longer 50-70 minute interactions (T_{long}). During interactions TCs remain stationary. Antigenic signal is presented by the DCs in the form of representative values of MHCI or MHCII (), and decays with time (t) with the form :

$$MHCI(t) = MHCI_i(0.5)^{\frac{t}{MHCI_{\frac{1}{2}}}} \tag{1}$$

$MHCII_i$ is the initial MHCI or initial MHCII presented with respective MHC half-lives $MHCI_{1/2}$ and $MHCII_{1/2}$ estimated from *in-vitro* labelling of MHC molecules [19–22]. During cognate TC-DC interaction, $CD4^+/CD8^+$ TCs gain (S) at rate κs while losing stimulation at rate λS (Fig B.iii).Total change in TC stimulation is therefore given according to the first order rate equation:

$$\frac{dS}{dt} = K_s\ MHCII(t) - \lambda_S\ S(t) \tag{2}$$

Accumulated simulation decays to a minimal value of S=1 to allow differentiation between cognate TCs that gain and lose simulation (S=1) and those that never gain simulation (S=0). Probability of cognate CD_{4^+}activation (P_{a4^+}) or cognate CD_{8^+}activation (P_{a8^+}) is calculated with a sigmoidal function given by:

$$P_{a4^+} = \frac{1}{1 + e^{\frac{-S - Act\mu_4}{Actl_4}}} \tag{3}$$

Parameter Actμ_4 determines the value of S required for 50% probability of activation and Actl_4 determines steepness of sigmoid inflection (Fig A.iv). Activation probability for $CD8^+$ TCs (P_{a8^+}) is determined with a sigmoid curve using a lower inflection point, (Actμ_8), than for $CD4^+$ TCs. However, if the DC is 'licenced', which occurs post-interaction with an activated $CD4^+$ TC, $CD8^+$ TC and $CD4^+$ TC stimulation requirements are equal. This is to reflect facilitated $CD8^+$ activation as a result of activated $CD4^+$ induced production of cytokines [23]. Model parameters were estimated such that TC activation became apparent 8-15 hours post DC-arrival [24–26]. This method of signal integration and the subsequent progressive patterns of TC proliferation and differentiation is supported by *in-vivo* observations and modelling descriptions [26–29]. It is assumed that co-stimulatory requirements are met as agDCs are highly efficient antigen-presenting cells.

Post-activation, proliferation is possible every 11 ($CD4^+$) or 9 ($CD8^+$) $\pm$1hr [30–33]. Differentiation to effector or memory TCs is possible after >=4 divisions, with differentiation probability determined with a second set of sigmoidal probability curves with midpoint $Dif\mu_{4+}$ and $Dif\mu_{8+}$ respectively [34,35]. Greater $CD4^+$ TCs dependence on continued stimulation for differentiation than $CD8^+$ TCs was implemented by using a higher minimum threshold of accumulated stimulation for $CD4^+$ differentiation than for $CD8^+$ TCs [36–40]. The fraction of effector TCs that differentiate into memory TCs increases from 0.01 to 0.04 as TCs progress from 'early effectors' (< 8 proliferations) to 'late effectors' [41]. This was implemented by assigning differentiation ratios of dif_{early} and dif_{late} to the two subsets.

1.5 T cell egress

When a T cell enters an exit area, the probability that it may egress (P_e) is calculated by multiplying a factor representing each T cell's $S1P_1r$ expression (SP) by a exit probability (E). Naive T cells have default SP value of 1, and E was experimentally determined under non-inflammatory conditions to produce T cell influx and egress equilibrium.

Change in relative $S1P_1r$, from a default of SP=1 expressed by naive TCs, was considered and estimated in three scenarios, using *in-vivo* and *in-vitro* observations [42–44]. Firstly, $S1P_1r$ is temporarily down-regulated (4 hours) following TC migration into the paracortex from the blood, due to the change from a high SP to low SP concentration environment. This is applied by tracking the time since each T cell entered (in an internal property), and setting SP equal to SP_{in}. Secondly, LN shutdown is triggered with sufficient increase in paracortical inflammatory state, determined by summation of MHC signal present, and a non-specific decrease in $S1P_1r$ expression occurs ($SP=SP_{inflam}$) until the inflammatory signal subsides. Thirdly $S1P_1r$ is down-regulated on activated TCs (SP_{act}) and gradually re-expressed on effector TCs (SP_{early}, SP_{late}) (Fig B) .

Fig B Modelling Sphingosine-1-phospate-1 receptor ($S1P_1r$)-mediated retention. Regulation of $S1P_1r$ on (i) naïve TCs post-transmigration from the blood, (ii) naïve TCs during LN shutdown due to detection of inflammatory signals and (iii) activated and early effector TCs.

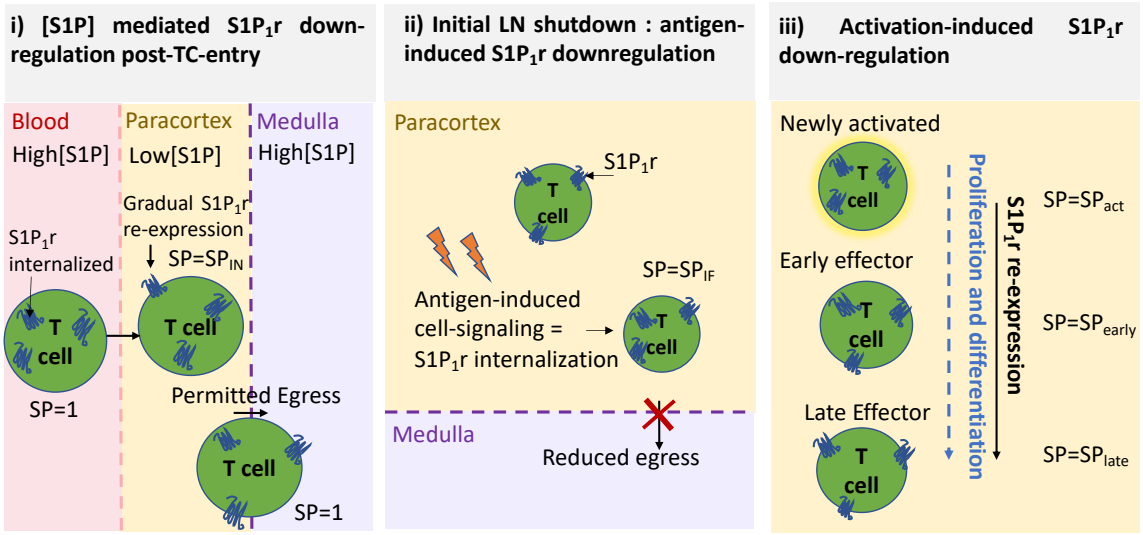

Model Structure

The model was built using a class based structure, depicted in Fig C. The 'Constants' class stores initialisation values and constant properties. The 'ContextBuilder' file creating a single copy of the Grid and/or Continuous Space - setting the environment up before adding copies of the agents (T cell and DC classes). A GridCell class allows definition of grid compartments at each gridpoint. A 'valueLayer' is also created, which is a parallel grid that we used to store properties of each grid compartment (see 1.1). Agents created using the classes as templates and positioned by assigning grid point coordinates (See Builder file). After initial set up, the 'context' file contains the counters and functions called every time step.

Fig C A class diagram displaying the underlying ABM structure.

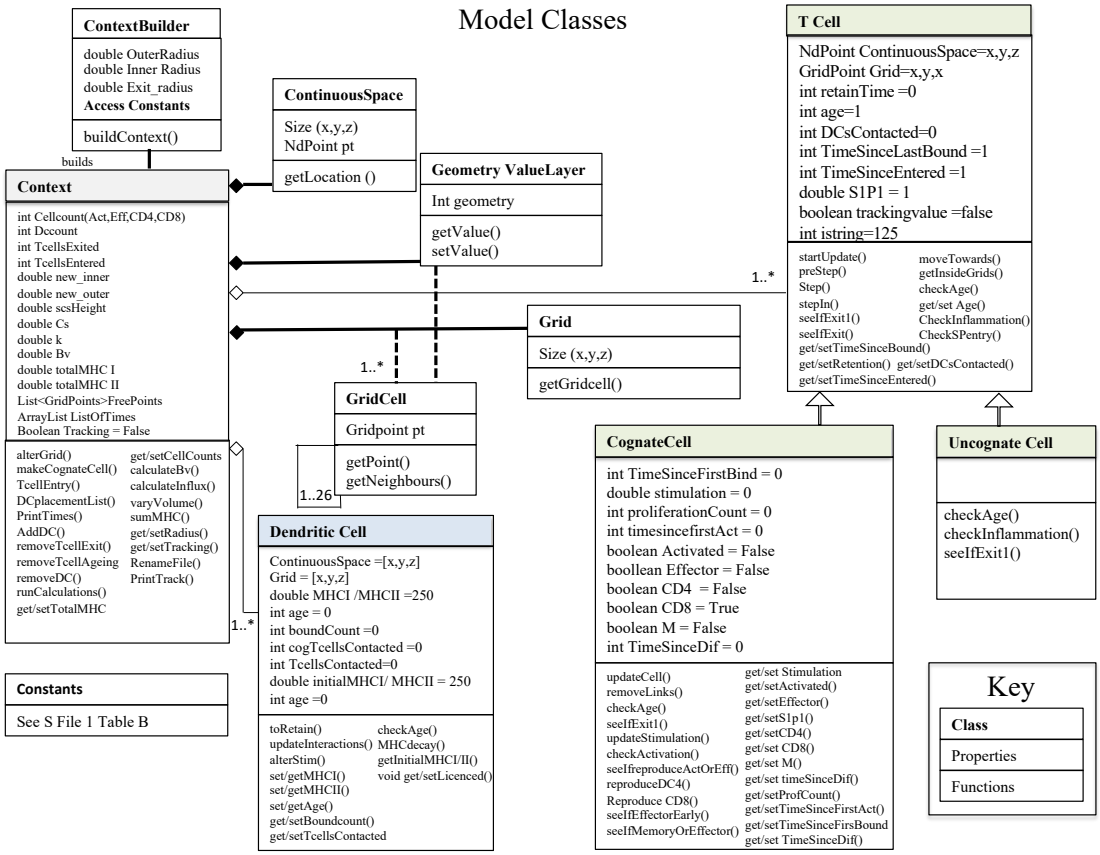

The are two agent classes - T cells and DCs. Two sub-classes - CognateCell and UncognatCell inherit properties and functions from the T cell class, alongside additional properties and/or functions. It is unneccesary for activation properties, and information about the type of cell (eg. CD4+/CD8+) to be stored in unCognate cells as only cognate TCs will respond to antigenic stimuli.

T cell properties include counters updated each timestep, such as 'timeSinceEntered', set at 1 when TCs enter, to implement S1P1r down-regulation on newly entered T cells. However, T cells that are present on initialisation have timeSinceEntered set at 0 and are never updated. An equilibrium

'timeSinceLastBound' are adjusted during interactions with DCs. Cognate T cells store additional properties related to activation state and stimulation level. DC properties include age, licensing state, history of interactions, current MHC level and current number of TCs bound. Interaction between TCs and DCs is applied by creating projections (links). Both ends of the link (eg. DC and TC) can be accessed via functions in either agent class and agent properties are used to record interaction duration, interaction history and T cell type, to determine remaining interaction duration.

The 'context' class initiates the main functions, described in Figure 2B, that are called each time. The rules and cell behaviour described in the methods above are integrated within these functions and sub-functions explained in S2 File. The class files have also been annotated.

Running the model in RepastSimphony

RepastSimphony is available at repast.github.io/.Our code can be downloaded from github.com/johnsara04/paracortex_model_johnson19 and the LN_simple5 package imported into repast symphony. The individual class files are located under '/LN_simple5/src/lN_simple5'. To run the model, once imported, the model with a visual interface can be initiated by clicking the down arrow next to the the green play button and selecting LN5_simple model. However, we recommend using the batch lnSimple5 option without a visual interface for speed. The default batch method uses the capacity of the local machine but we used an external high performance computing (HPC) system. This involved generating a jar file containing the necessary model classes and transferring to a HPC system (see Fig D) pre-installed with repastSimphony and a java development kit. We also edited the configuration file and manually added a Jobscript file containing instructions to run simulations on a PBS batch system. The repast documentation has since been updated to accurately explain how to run a batch simulation using an EC2 instance on Amazon Web Services, in a manner that avoids file transfer and manual JobScript editing, which we would recommend as an effective batch simulation method-
see repast.github.io/docs/RepastBatchRunsGettingStarted.pdf.

Fig D The process of generating the model for batch simulations. We used an external HPC system with RepastSimphony and a Java-development-kit installed. We generated locally a jar-file containing the model classes, required libraries and parameters and transferred this along with a configuration file and a PBS jobscript file containing run and output instructions to our HPC instance. Output was transferred back to our local computer and data analysis performed in Matlab.

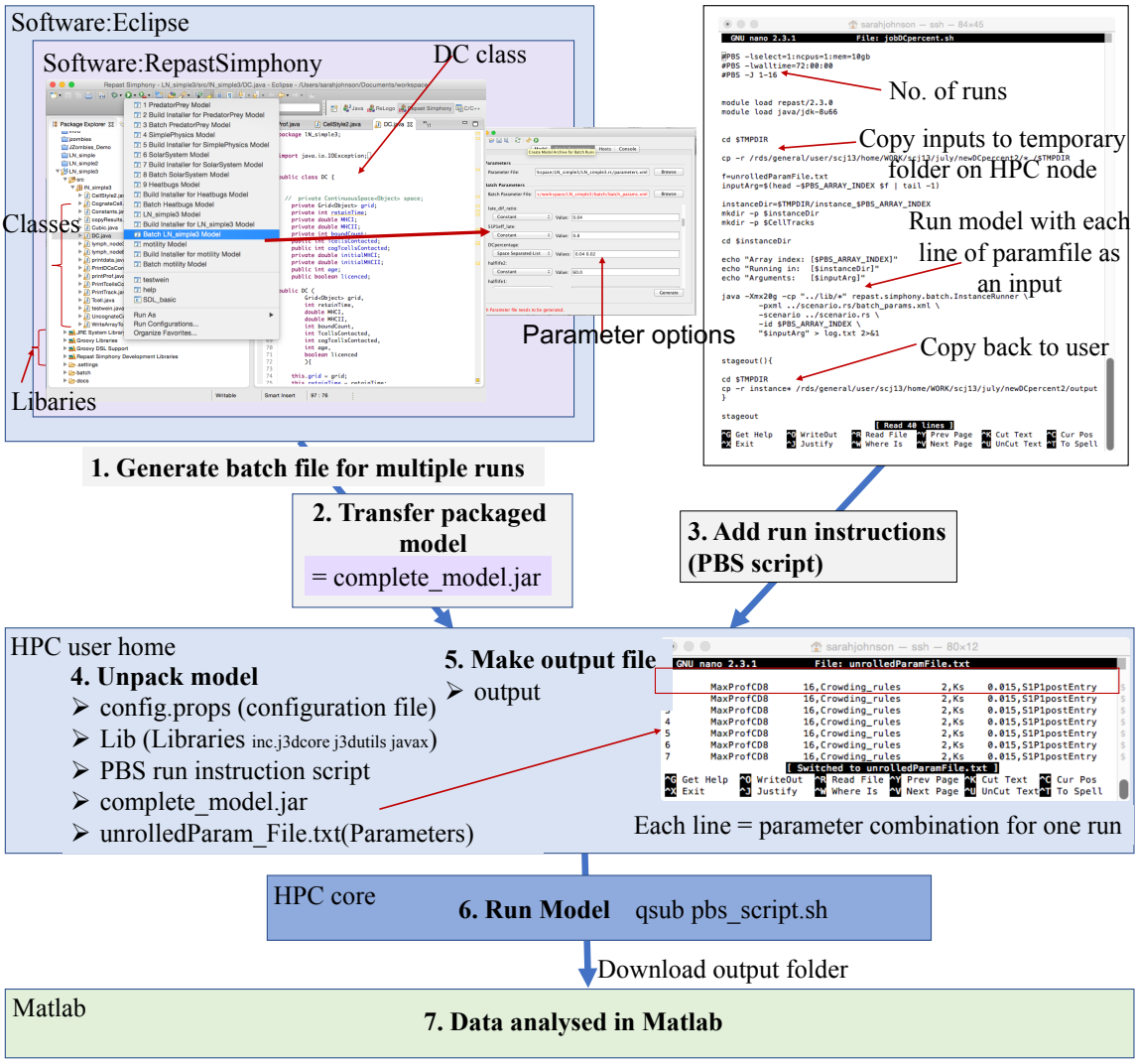

S1 File Supplementary Parameter Tables

Table B Parameters and properties that were not varied in the global sensitivity analysis

Symbol	Parameter	Value	Reference
	Model Geometry		
r_p	Initial paracortex radius	200μm	[45, 46]
-	Entry radius	0.5 r_p	[1]
-	Afferent entry radius	0.3 r_p	[1]
-	Exit radius	0.07r_p	[45, 46]
-	Sub Capsular Sinus height	0.7r_p	[45, 46]
GS	Grid Size	6μm	-
	TC Properties		
-	Initial occupation	55%	[47]
-	Radius	3.3μm	[48]
-	Ratio CD4:CD8	0.7:0.3	[45, 46]
-	Lifespan naive	365 days	[49, 50]
-	Lifespan activated	41 hours	[49, 50]
-	Lifespan effectors	3.5 days	[49, 50]
-	TC entry Afferent:HEV ratio	0.1:0.9	[51, 52]
Actl_{4+}	Slope of CD4$^+$ activation curve	-69.81	-
Actl_{8+}	Slope of CD4$^+$ activation curve	-80.71	-
Difl_{4+}	Slope of CD4$^+$ differentiation curve	-17.26	-
Difl_{8+}	Slope of CD8$^+$ differentiation curve	-13.58	-
	T cell movement		
β	Probability of movement	0.6	[1, 34, 53–55]
P_e	Probability of egress constant	0.0126	-
γ	Max cells per grid	2	-
T_{res}	TC residence time	24hrs	[13, 56]
	DC properties		
-	DC span	2 grids	[48, 57, 58]
-	DC Lifespan	60 hours	[2, 59, 60]

Table C Parameters varied in the global sensitivity analysis. Continued overleaf.

Symbol	Parameter Description	Default	Min	Max	Mean	SD	Distrib.	Ref
	TC response parameters							
$Act\mu_4$	$CD4^+$ activation curve mean	120	70	230	-	-	Unif	[61–66]
$Act\mu_8$	$CD8^+$ activation curve mean	140	90	250	-	-	Unif	[61–66]
$Dif\mu_4$	$CD4^+$ differentiation curve mean	60	30	90	-	-	Unif	[61–66]
$Dif\mu_8$	$CD8^+$ differentiation curve mean	40	20	60	-	-	Unif	[61–66]
TP_4	Min time between $CD4^+$ proliferations (hrs)	11	-	-	11	1.16	Norm	[30–33]
TP_8	Min time between $CD8^+$ proliferations (hrs)	7	-	-	7	0.88	Norm	[30, 31]
Max_{P8}	Max proliferations $CD8^+$	16	-	-	16	1.2	Norm	[39, 67–69]
Max_{P4}	Max proliferations $CD4^+$	10	-	-	10	1.2	Norm	[31–33]
Dif_{early}	Early Memory:Effector cell differentiation	0.01	0.001	0.02	0.01	-	Exp	[70]
Dif_{late}	Late Memory:Effector cell differentiation	0.04	0.01	0.08	-	-	Unif	[70]
	TC interaction dynamics							
T_{NC}	Mean non-cognate T-DC interaction (min)	3.5	-	-	3.5	1	Norm	[60, 71]
T_{short}	Short cognate TC-DC interaction (min)	10-15	-	-	10	3	Norm	[25, 60, 71]
T_{long}	Long cognate TC-DC interaction (min)	50-70	-	-	50	12	Norm	[24–26, 72]
T_{change}	Time TCs switch to long interactions (hr)	8	-	-	8	1	Norm	[24–26, 72]
B_{max}	Max TCs a DC can bind per-step	3	1	5	-	-	Unif	-
B_{step}	Max TCs a DC can bind	15	4	20	-	-	Unif	[73]
	TC Stimulation							
K_s	Stim. gain coefficient	0.015	0.005	0.02	-	-	Unif	-
λ	TC stim. decay factor	0.99	0.99545	0.9999	-	-	Unif	-
MHC_i	Initial MHCI/II	250	150	350	-	-	Unif	[19–22]
$MHCI_{1/2}$	MHCI half life (hrs)	19.7	-	-	19.7	6	Norm	[19, 20]
$MHCII_{1/2}$	MHCII half life (hrs)	60	-	-	60	6	Norm	[21, 22]
F_{cog}	Frequency of cognate TCs that enter	1e-4	5e-5	1.5e-4	-	-	Unif	[32, 74–76]
Φ_{DC}	Total DCs entering as % of initial TCs	0.04	0.02	0.06	-	-	Unif	[2]
T_{DCin}	DC entry duration (days)	2.5	0.5	4.5	-	-	Unif	[2]

Symbol	Parameter Description	Default	Min	Max	Mean	SD	Distrib.	Ref
	Sphingosine-1-phosphate receptor regulation							
SP_{entry}	$S1P_1r$ expression post entry	0.1	0.01	1	-	-	Unif	[42,43,77]
SP_{act}	$S1P_1r$ expression when activated	0.01	0.001	0.02	-	-	Unif	[42-44,77]
$S1_{early}$	Effector $S1P_1r$ (Proliferation<=6)	0.4	0.01	1	-	-	Unif	[42,44]
SP_{late}	Effector $S1P_1r$ (Proliferation>6)	0.8	0.3	1.3	-	-	Unif	[42,44]
SP_{mem}	Memory $S1P_1rr$	1	-	-	1	0.1	Norm	[42,44]
SP_{IF}	$S1P_1r$ on all TCs during inflam.	0.4	0.2	0.8	-	-	Unif	-
T_{Entry}	Time $S1P_1rr$ is low post-entry (min)	60	13	120	-	-	Unif	-
T_{Inflam}	Time to alter $S1P_1r$ during inflam.(hr)	4	1	7.5	-	-	Unif	-
	T cell recruitment							
RT1	recruitment increase stim. threshold	2e4	2e4	1e5	-	-	Unif	[5,7,78,79]
RT2	Stim. threshold for max. recruitment	4e5	2e5	2e6	-	-	Unif	[5,7,78,79]
R_F	Recruitment Factor	3e-6	1e-6	4e-6	-	-	Unif	[5,7,78,79]
	Paracortex expansion							
V_{Max}	Max fold-volume increase	1.00	2.00	2.50	-	-	Unif	-
l	Rate of volume change around m	7e-05	3e-05	1e-04	-	-	Unif	-
T_{mid}	No. of TCs for 50% max-volume	120000	90000	150000	-	-	Unif	-

References

[1] Girard JP, Moussion C, Förster R. HEVs, lymphatics and homeostatic immune cell trafficking in lymph nodes. Nat Rev Immunol. 2012;12(11):762–73.

[2] Acton SE, Farrugia AJ, Astarita JL, Mourao-Sa D, Jenkins RP, Nye E, et al. Dendritic cells control fibroblastic reticular network tension and lymph node expansion. Nature. 2014 10;514(7523):498–502.

[3] Kumar V, Chyou S, Stein J, Lu T. Optical projection tomography reveals dynamics of HEV growth after immunization with protein plus CFA and features shared with HEVs in acute. Frontiers in immunology. 2012;7(3):282.

[4] Kumar V, Scandella E, Danuser R, Onder L, Nitschké M, Fukui Y, et al. Global lymphoid tissue remodeling during a viral infection is orchestrated by a B cell–lymphotoxin-dependent pathway. Blood. 2010;115(23):4725–4733.

[5] Webster B, Ekland EH, Agle LM, Chyou S, Ruggieri R, Lu TT. Regulation of lymph node vascular growth by dendritic cells. J Exp Med. 2006;203(8):1903–13.

[6] Tedla N, Wang H, HP M. Regulation of T lymphocyte trafficking into lymph nodes during an immune response by the chemokines macrophage inflammatory protein (MIP)-1 and MIP-1I2. The Journal of Imm. 1998;161(10):5663–72.

[7] Drayson MT, Smith ME. The sequence of changes in blood flow and lymphocyte influx to stimulated rat lymph nodes. Immunology. 1981;44:125–133.

[8] Soderberg KA, Payne GW, Sato A, Medzhitov R, Segal SS, Iwasaki A. Innate control of adaptive immunity via remodeling of lymph node feed arteriole. Proceedings of the National Academy of Sciences of the United States of America. 2005 5;102(45):16315–16320.

[9] Yang CYY, Vogt TK, Favre S, Scarpellino L, Huang HYY, Tacchini-Cottier F, et al. Trapping of naive lymphocytes triggers rapid growth and remodeling of the fibroblast network in reactive murine lymph nodes. PNAS. 2014;111(1):E109–18.

[10] Cahill R, Frost H, Trnka Z. The effects of antigen on the migration of recirculating lymphocytes through single lymph nodes. J Exp Med. 1976;143(4):870–888.

[11] Habenicht LM, Albershardt TC, Iritani BM, Ruddell A. Distinct mechanisms of B and T lymphocyte accumulation generate tumor-draining lymph node hypertrophy. Oncoimmunology. 2016 08;5(8):e1204505.

[12] Battaglia A, Ferrandina G, Buzzonetti A, Malinconico P, Legge F, Salutari V, et al. Lymphocyte populations in human lymph nodes. Alterations in CD4(+) CD25(+) T regulatory cell phenotype and T-cell receptor Beta-repertoire. Immunology. 2003 11;110(3):304–312.

[13] Tomura M, Yoshida N, Tanaka J. Monitoring cellular movement in vivo with photoconvertible fluorescence protein 'Kaede' transgenic mice. PNAS. 2008;105(31):10871–6.

[14] Latif R, de Rosbo NK, Amarant T, Rappuoli R, Sappler G, Ben-Nun A. Reversal of the CD4(+)/CD8(+) T-Cell Ratio in Lymph Node Cells upon In Vitro Mitogenic Stimulation by Highly Purified, Water-Soluble S3-S4 Dimer of Pertussis Toxin. Infection and Immunity. 2001 05;69(5):3073–3081. Available from: http://www.ncbi.nlm.nih.gov/pmc/articles/PMC98262/.

[15] Celli S, Day M, Müller AJ, Molina-Paris C, Lythe G, Bousso P. How many dendritic cells are required to initiate a T-cell response? Blood. 2012;120(19):3945–3948.

[16] Bogle G, Dunbar PR. Simulating T-cell motility in the lymph node paracortex with a packed lattice geometry. Imm Cell Biol. 2008 08;86(8):676–687.

[17] Brown LV, Gaffney EA, Wagg J, Coles MC. An in silico model of cytotoxic T-lymphocyte activation in the lymph node following short peptide vaccination. Journal of the Royal Society, Interface. 2018 03;15(140):2018.0041.

[18] Harris TH, Banigan EJ, Christian DA, Konradt C, Tait Wojno ED, Norose K, et al. Generalized Lévy walks and the role of chemokines in migration of effector CD8+ T cells. Nature. 2012 05;486:545–548.

[19] Cella M, Salio M, Sakakibara Y, Langen H, Julkunen I, Lanzavecchia A. Maturation, Activation, and Protection of Dendritic Cells Induced by Double-stranded RNA. The Journal of Experimental Medicine. 1999 03;189(5):821–829.

[20] Kukutsch NA, Rossner S, Austyn JM, Schuler G, Lutz MB. Formation and Kinetics of MHC Class I-Ovalbumin Peptide Complexes on Immature and Mature Murine Dendritic Cells. Journal of Investigative Dermatology. 2000;115(3):449 – 453.

[21] Cella M, Engering A, Pinet V, Pieters J, Lanzavecchia A. Inflammatory stimuli induce accumulation of MHC class II complexes on dendritic cells. Nature. 1997 08;388:782–7.

[22] Baumgartner C, Ferrante A, Nagaoka M, Gorski J, Malherbe LP. Peptide-MHC Class II Complex Stability Governs CD4 T Cell Clonal Selection. Journal of immunology (Baltimore, Md : 1950). 2010 01;184(2):573–581.

[23] Smith CM, Wilson NS, Waithman J, Villadangos JA, Carbone FR, Heath WR, et al. Cognate CD4+ T cell licensing of dendritic cells in CD8+ T cell immunity. Nature Immunology. 2004 10;5:1143–8.

[24] Hugues S, Fetler L, Bonifaz L, Helft J, Amblard F, Amigorena S. Distinct T cell dynamics in lymph nodes during the induction of tolerance and immunity. Nature Immunology. 2004 10;5:1235–42.

[25] Mempel TR, Henrickson SE, Von Andrian UH. T-cell priming by dendritic cells in lymph nodes occurs in three distinct phases. Nature. 2004;427(6970):154–9.

[26] Stoll S, Delon J, Brotz T, Germain R. Dynamic imaging of T cell-dendritic cell interactions in lymph nodes. Science. 2002;296(5574):1873–6.

[27] Germain RN, Stefanová I. THE DYNAMICS OF T CELL RECEPTOR SIGNALING: Complex Orchestration and the Key Roles of Tempo and Cooperation. Annual Review of Immunology. 1999 07;17(1):467–522.

[28] Rachmilewitz J, Lanzavecchia A. A temporal and spatial summation model for T-cell activation: signal integration and antigen decoding. Trends in Immunology. 2002;23(12):592–595.

[29] Lanzavecchia A, Sallusto F. Progressive differentiation and selection of the fittest in the immune response. Nature Reviews Immunology. 2002 12;2:982–7.

[30] De Boer RJ, Homann D, Perelson AS. Different Dynamics of CD4+ and CD8+ T Cell Responses During and After Acute Lymphocytic Choriomeningitis Virus Infection. The Journal of Immunology. 2003;171(8):3928–3935.

[31] Foulds KE, Zenewicz LA, Shedlock DJ, Jiang J, Troy AE, Shen H. Cutting Edge: CD4 and CD8 T Cells Are Intrinsically Different in Their Proliferative Responses. The Journal of Immunology. 2002;168(4):1528–1532.

[32] Nelson RW, Beisang D, Tubo NJ, Dileepan T, Wiesner DL, Nielsen K, et al. T cell receptor cross-reactivity between similar foreign and self peptides influences naïve cell population size and autoimmunity. Immunity. 2015 01;42(1):95–107.

[33] Tubo NJ, Pagán AJ, Taylor JJ, Nelson RW, Linehan JL, Ertelt JM, et al. Single Naive CD4$^+$ T Cells from a Diverse Repertoire Produce Different Effector Cell Types during Infection. Cell. 2013 04;153(4):785–796.

[34] Miller MJ, Wei SH, Parker I, Cahalan MD. Two-photon imaging of lymphocyte motility and antigen response in intact lymph node. Science. 2002;296(5574):1869–73.

[35] Linderman JJ, Riggs T, Pande M, Miller M, Marino S, Kirschner DE. Characterizing the Dynamics of CD4+ T Cell Priming within a Lymph Node. The Journal of Immunology. 2010;184(6):2873–2885.

[36] Schrum AG, Palmer E, Turka LA. Distinct temporal programming of naive CD4(+) T cells for cell division versus TCR-dependent death susceptibility by antigen-presenting macrophages. European journal of immunology. 2005 02;35(2):449–459.

[37] Wong P, Pamer EG. Cutting Edge: Antigen-Independent CD8 T Cell Proliferation. The Journal of Immunology. 2001;166(10):5864–5868.

[38] Kaech SM, Ahmed R. Memory CD8+ T cell differentiation: initial antigen encounter triggers a developmental program in naïve cells. Nature Immunology. 2001 05;2:415–22.

[39] van Stipdonk MJB, Lemmens EE, Schoenberger SP. Naïve CTLs require a single brief period of antigenic stimulation for clonal expansion and differentiation. Nature Immunology. 2001 05;2:423–9.

[40] Shaulov A, Murali-Krishna K. CD8 T Cell Expansion and Memory Differentiation Are Facilitated by Simultaneous and Sustained Exposure to Antigenic and Inflammatory Milieu. The Journal of Immunology. 2008;180(2):1131–1138.

[41] Obar JJ, Khanna KM, Lefrançois L. Endogenous naive CD8+ T cell precursor frequency regulates primary and memory responses to infection. Immunity. 2008 06;28(6):859–869. Available from: https://www.ncbi.nlm.nih.gov/pubmed/18499487.

[42] Pham T, Okada T, Matloubian M, Lo C, Cyster J. S1P 1 receptor signaling overrides retention mediated by Gi-coupled receptors to promote T cell egress. Immunity. 2008;28(1):122–133.

[43] Matloubian M, Lo C, Cinamon G, Lesneski M, Xu Y. Lymphocyte egress from thymus and peripheral lymphoid organs is dependent on S1P receptor 1. Nature. 2004;427(6972):355–60.

[44] Garris CS, Blaho VA, Hla T, Han MH. Sphingosine-1-phosphate receptor 1 signalling in T cells: trafficking and beyond. Immunology. 2014 07;142(3):347–353.

[45] Mueller SN, Germain RN. Stromal cell contributions to the homeostasis and functionality of the immune system. Nature Reviews Immunology. 2009 07;9:618–29.

[46] Kuka M, Iannacone M. The role of lymph node sinus macrophages in host defense. Annals of the New York Academy of Sciences. 2014;1319(1):38–46.

[47] He Y. Scanning electron microscope studies of the rat mesenteric lymph node with special reference to high-endothelial venules and hitherto unknown lymphatic labyrinth. Archivum histologicum Japonicum. 1985;(48):1–15.

[48] Tasnim H, Fricke GM, Byrum JR, Sotiris JO, Cannon JL, Moses ME. Quantitative Measurement of Naïve T Cell Association With Dendritic Cells, FRCs, and Blood Vessels in Lymph Nodes. Frontiers in Immunology. 2018;9:1571.

[49] Tough DF, Sprent J. Life span of naive and memory t cells. STEM CELLS. 1995;13(3):242–249.

[50] Sprent J, Tough DF. T Cell Death and Memory. Science. 2001;293(5528):245–248.

[51] Smith JB, McIntosh GH, Morris B. The traffic of cells through tissues: a study of peripheral lymph in sheep. Journal of Anatomy. 1970 07;107(Pt 1):87–100.

[52] Hall J, Morris B. The immediate effect of antigens on the cell output of a lymph node. British journal of experimental pathology. 1965;46(4):450–454.

[53] Park E, Peixoto A, Imai Y, Goodarzi A, Cheng G. Distinct roles for LFA-1 affinity regulation during T-cell adhesion, diapedesis, and interstitial migration in lymph nodes. Blood. 2010;115(8):1572–81.

[54] Boscacci R, Pfeiffer F, Gollmer K, Sevilla A. Comprehensive analysis of lymph node stroma-expressed Ig superfamily members reveals redundant and nonredundant roles for ICAM-1, ICAM-2, and VCAM-1 in lymphocyte homing. Blood. 2010;116(6):915–25.

[55] Park C, Hwang I, Sinha R, Kamenyeva O. Lymph node B lymphocyte trafficking is constrained by anatomy and highly dependent upon chemo-attractant desensitization. Blood. 2012;119(4):978–989.

[56] Catron DM, Itano AA, Pape KA, Mueller DL, Jenkins MK. Visualizing the first 50 hr of the primary immune response to a soluble antigen. Immunity. 2004;21(3):341–347.

[57] Nitschké M, Aebischer D, Abadier M, Haener S, Lucic M, Vigl B, et al. Differential requirement for ROCK in dendritic cell migration within lymphatic capillaries in steady-state and inflammation. Blood. 2012;120(11):2249–2258.

[58] Paharkova-Vatchkova V, Maldonado R, Kovats S. Estrogen Preferentially Promotes the Differentiation of CD11c+ CD11bintermediate Dendritic Cells from Bone Marrow Precursors. The Journal of Immunology. 2004;172(3):1426–1436.

[59] Kamath AT, Henri S, Battye F, Tough DF, Shortman K. Developmental kinetics and lifespan of dendritic cells in mouse lymphoid organs. Blood. 2002;100(5):1734–1741.

[60] Bousso P. T-cell activation by dendritic cells in the lymph node: lessons from the movies. Nature Reviews Immunology. 2008 09;8:675–84.

[61] Bajénoff M, Granjeaud S, Guerder S. The strategy of T cell antigen-presenting cell encounter in antigen-draining lymph nodes revealed by imaging of initial T cell activation. Journal of Experimental Med. 2003;198(5):715–724.

[62] Yoon H, Legge KL, Sung SsJ, Braciale TJ. Sequential Activation of CD8+ T Cells in the Draining Lymph Nodes in Response to Pulmonary Virus Infection. The Journal of Immunology. 2007;179(1):391–399.

[63] Lawrence CW, Braciale TJ. Activation, Differentiation, and Migration of Naive Virus-Specific CD8+ T Cells during Pulmonary Influenza Virus Infection. The Journal of Immunology. 2004;173(2):1209–1218.

[64] Demotz S, Grey H, Sette A. The minimal number of class II MHC-antigen complexes needed for T cell activation. Science. 1990;249(4972):1028–1030.

[65] Lee WT, Pasos G, Cecchini L, Mittler JN. Continued Antigen Stimulation Is Not Required During CD4+ T Cell Clonal Expansion. The Journal of Immunology. 2002;168(4):1682–1689.

[66] Arens R, Schoenberger SP. Plasticity in programming of effector and memory CD8(+) T-cell formation. Immunological reviews. 2010 05;235(1):190–205.

[67] Butz EA, Bevan MJ. Massive Expansion of Antigen-Specific CD8(+) T Cells during an Acute Virus Infection. Immunity. 1998 02;8(2):167–175.

[68] Murali-Krishna K, Altman JD, Suresh M, Sourdive DJD, Zajac AJ, Miller JD, et al. Counting Antigen-Specific CD8 T Cells: A Reevaluation of Bystander Activation during Viral Infection. Immunity. 1998 07;8(2):177–187.

[69] Busch DH, Pilip IM, Vijh S, Pamer EG. Coordinate Regulation of Complex T Cell Populations Responding to Bacterial Infection. Immunity. 1998 07;8(3):353–362.

[70] Williams MA, Bevan MJ. Shortening the Infectious Period Does Not Alter Expansion of CD8 T Cells but Diminishes Their Capacity to Differentiate into Memory Cells. The Journal of Immunology. 2004;173(11):6694–6702.

[71] Miller MJ, Hejazi AS, Wei SH, Cahalan MD, Parker I. T cell repertoire scanning is promoted by dynamic dendritic cell behavior and random T cell motility in the lymph node. Proc Natl Acad Sci USA. 2004;101(4):998–1003.

[72] von Andrian U, Mackay C. T-cell function and migration, two sides of the same coin. New England Journal of Medicine. 2000;343(14):1020–34.

[73] Bousso P, Robey E. Dynamics of CD8+ T cell priming by dendritic cells in intact lymph nodes. Nature immunology. 2003;4:579–585.

[74] Laouini D, Casrouge A, Dalle S, Lemonnier F, Kourilsky P, Kanellopoulos J. VI2 T Cell Repertoire of CD8+ Splenocytes Selected on Nonpolymorphic MHC Class I Molecules. The Journal of Immunology. 2000;165(11):6381–6386.

[75] Blattman JN, Antia R, Sourdive DJ, Wang X, Kaech SM, Murali-Krishna K, et al. Estimating the Precursor Frequency of Naive Antigen-specific CD8 T Cells. The Journal of Experimental Medicine. 2002 03;195(5):657–664.

[76] Jenkins MK, Moon JJ. The role of naïve T cell precursor frequency and recruitment in dictating immune response magnitude. Journal of Immunology (Baltimore, Md : 1950). 2012 05;188(9):4135–4140.

[77] Lo C, Xu Y, Proia R, Cyster J. Cyclical modulation of sphingosine-1-phosphate receptor 1 surface expression during lymphocyte recirculation and relationship to lymphoid organ transit. Journal of Experimental Medicine. 2005;2(201):291–301.

[78] Hay JB, Hobbs BB. The flow of blood to lymph nodes and its relation to lymphocyte traffic and the immune response. Journal of Experimental Medicine. 1977;145(1):31–44.

[79] Mackay C, Marston W, Dudler L. Altered patterns of T cell migration through lymph nodes and skin following antigen challenge. European journal of Imm. 1992;22(9):2205–10.